REGULAR ARTICLE

blood advances

Genetic barcoding systematically compares genes in del(5q) MDS and reveals a central role for *CSNK1A1* in clonal expansion

Ursula S. A. Stalmann,[1,2] Fabio Ticconi,[3] Inge A. M. Snoeren,[1,2] Ronghui Li,[3] Hélène F. E. Gleitz,[1,2] Glenn S. Cowley,[4] Marie E. McConkey,[5] Aaron B. Wong,[6] Stephani Schmitz,[1,2] Stijn N. R. Fuchs,[1,2] Shubhankar Sood,[7,8] Nils B. Leimkühler,[2] Sergio Martinez-Høyer,[2] Bella Banjanin,[1,2] David Root,[4] Tim H. Brümmendorf,[9] Juliette E. Pearce,[10] Andreas Schuppert,[11] Eric M. J. Bindels,[12] Marieke A. Essers,[7,8] Dirk Heckl,[13] Thomas Stiehl,[14] Ivan G. Costa,[3,*] Benjamin L. Ebert,[5,15,*] and Rebekka K. Schneider[1,2,10,*]

[1]Department of Developmental Biology and [2]Oncode Institute, Erasmus Medical Center Cancer Institute, Rotterdam, The Netherlands; [3]Institute for Computational Genomics, Faculty of Medicine, Rheinisch-Westfälische Technische Hochschule (RWTH) Aachen University, Aachen, Germany; [4]Broad Institute of Harvard University and Massachusetts Institute of Technology, Cambridge, MA; [5]Department of Medical Oncology, Dana-Farber Cancer Institute, Boston, MA; [6]Department of Neuroscience, Erasmus Medical Center, Rotterdam, The Netherlands; [7]German Cancer Research Center (DKFZ), Heidelberg, Germany; [8]Heidelberg Institute for Stem Cell Technology and Experimental Medicine (HI-STEM GMBH), Heidelberg, Germany; [9]Department of Hematology, Oncology, Hemostaseology, and Stem Cell Transplantation, [10]Department of Cell Biology, Institute for Biomedical Engineering, Faculty of Medicine, and [11]Joint Research Center for Computational Biomedicine, RWTH Aachen University, Aachen, Germany; [12]Department of Hematology, Erasmus Medical Center Cancer Institute, Rotterdam, The Netherlands; [13]Pediatric Hematology and Oncology, Martin Luther University Halle-Wittenberg, Halle, Germany; [14]Institute for Computational Biomedicine-Disease Modeling, Faculty of Medicine, RWTH Aachen University, Aachen, Germany; and [15]Howard Hughes Medical Institute, Boston, MA

Key Points

- *Csnk1a1* haploinsufficient hematopoietic stem cells outcompete other key genes in del(5q) MDS in direct competitive transplantation.
- Chronic inflammatory stress increases the competitive advantage of *Csnk1a1* haploinsufficient hematopoietic stem cells.

How genetic haploinsufficiency contributes to the clonal dominance of hematopoietic stem cells (HSCs) in del(5q) myelodysplastic syndrome (MDS) remains unresolved. Using a genetic barcoding strategy, we performed a systematic comparison on genes implicated in the pathogenesis of del(5q) MDS in direct competition with each other and wild-type (WT) cells with single-clone resolution. *Csnk1a1* haploinsufficient HSCs expanded (oligo)clonally and outcompeted all other tested genes and combinations. *Csnk1a1*$^{-/+}$ multipotent progenitors showed a proproliferative gene signature and HSCs showed a downregulation of inflammatory signaling/immune response. In validation experiments, *Csnk1a1*$^{-/+}$ HSCs outperformed their WT counterparts under a chronic inflammation stimulus, also known to be caused by neighboring genes on chromosome 5. We therefore propose a crucial role for *Csnk1a1* haploinsufficiency in the selective advantage of 5q-HSCs, implemented by creation of a unique competitive advantage through increased HSC self-renewal and proliferation capacity, as well as increased fitness under inflammatory stress.

Introduction

Deletion of the long arm of chromosome 5 (del(5q)) is the most common cytogenetic aberration in myelodysplastic syndromes (MDSs).[1-3] Del(5q) MDS is a malignant clonal disorder of hematopoiesis arising in a hematopoietic stem cell (HSC). HSCs acquire a deletion of 1 copy of the long arm of chromosome 5 (ie, haploinsufficiency of 5q). The 5q-haploinsufficient HSCs gain a clonal advantage in the bone

Submitted 31 August 2021; accepted 23 December 2021; prepublished online on *Blood Advances* First Edition 11 January 2022; final version published online 15 March 2022. DOI 10.1182/bloodadvances.2021006061.

*I.G.C., B.L.E., and R.K.S. contributed equally to this study.

Single-cell RNA sequencing data sets have been deposited in Gene Expression Omnibus (GEO) (accession number GSE165395).

Original data may be obtained by e-mail request to the corresponding author.

The full-text version of this article contains a data supplement.

© 2022 by The American Society of Hematology. Licensed under Creative Commons Attribution-NonCommercial-NoDerivatives 4.0 International (CC BY-NC-ND 4.0), permitting only noncommercial, nonderivative use with attribution. All other rights reserved.

marrow and outcompete normal hematopoiesis. A critical, yet unresolved question remains as to how genetic haploinsufficiency contributes to the clonal dominance of HSCs.

Extensive research over the past 3 decades has led to the identification of several candidate genes within the commonly deleted regions on chromosome 5, involved in disease pathophysiology. Comprehensive molecular analyses using SNP-A karyotyping, whole-exome sequencing, and targeted sequencing have revealed recurrent somatic mutations involving *CSNK1A1* and *G3BP1* in the commonly deleted regions. In the commonly retained region, *DDX41* is mutated in only a minority of myeloid neoplasms with del(5q), which indicates that these mutations are not required for the phenotype.[1-5] Thus, it has been proposed that haploinsufficiency of 1 or multiple genes is responsible for the disease phenotype and clonal expansion of 5q− HSCs.[6]

Conditional heterozygous inactivation of genes in murine models provides an excellent model system for recapitulating acquired genetic haploinsufficiency in vivo. Functional studies have revealed individual genes that contribute to the clinical phenotype of del(5q) MDS and affect HSC regulation by haploinsufficiency. In particular, genes involved in cell cycle regulation, such as *Csnk1a1*, *Egr1*, and *Apc*, have been shown to provide a growth advantage within the HSC compartment.[1,7-13] *Egr1* is a transcription factor involved in multiple cell proliferation pathways. Knockout of *Egr1* in the hematopoietic system leads to increased proliferation and mobilization of HSCs, and *Egr1* haploinsufficiency vastly accelerates the emergence of myeloid and lymphoid malignancies after DNA damage.[12,13] *Apc* haploinsufficiency leads to increased cycling, apoptosis, and expansion of short-term HSCs (ST-HSCs) but ultimately to exhaustion of the HSC pool.[8,9] Impaired erythropoiesis in del(5q) MDS has been linked to heterozygous deletion of *RPS14*.[14,15] *Rps14* haploinsufficiency, however, does not lead to a clonal advantage of HSCs. These studies demonstrated that del(5q) MDS is a contiguous gene syndrome, in which haploinsufficiency for more than 1 gene contributes to the phenotype.[16,17]

Both *Csnk1a1*[1] and *Apc*[8,18] are central regulators of β-catenin function and are inactivated in ∼95% of cases with del(5q) MDS. β-Catenin is a major driver of stem cell self-renewal and neoplasia in multiple cellular lineages. Besides HSC-intrinsic mechanisms in the clonal expansion of 5q− HSCs, growing evidence suggests that extrinsic, microenvironmental factors favor the expansion of 5q− HSCs.[19-21]

In del(5q) MDS, the question remains as to which gene or combination of genes contributes to the clonal advantage of HSCs and which molecular mechanisms are responsible. Examining the relative impact of multiple individual genes, alone and in combination, is cumbersome when using standard in vivo methodologies. Conventional competitive repopulation assays are limited by the fact that only 1 genotype can be transplanted against a competitor wild-type (WT) cell population. As these assays are strongly influenced by the variability in mice (eg, microenvironment and irradiation, among others), it is difficult to directly compare different genotypes with one another. In the present investigation, a genetic barcoding approach within the same microenvironment was used to assess a clonal advantage amid competing, genetically distinct cells with haploinsufficiency for the 5q− genes *Csnk1a1*, *Egr1*, and *Apc*.

Materials and methods

Animal studies

Csnk1a1 conditional knockout mice[1] and *Apc*$^{tm1tyi/j}$,[22] *Egr1*$^{tm1jmi/j}$,[23] and *Ctnnb1*^{tm2kem},[24] mice have been described previously. Compound haploinsufficiency was achieved by crossing the conditional knockout mice with each other and with *Mx1-Cre* mice. Details are supplied in the supplemental Methods.

Mouse experiments were performed according to an Institutional Animal Care and Use Committee–approved protocol at Children's Hospital Boston and protocols approved by the Central Animal Committee (Centrale Commissie Dierproeven [CCD], The Netherlands, under approval AVD1010020173387).

Competitive transplants

In competitive bone marrow transplantation studies, freshly isolated CD45.2$^+$ bone marrow cells were harvested, equally mixed with freshly isolated CD45.1$^+$ bone marrow competitor cells and transplanted into CD45.1$^+$-recipient mice. 4 weeks after transplantation, the excision was induced in the floxed genotypes crossed to *Mx1Cre*$^+$ by polyinosinic-polycytidylic acid (poly(IC)) injection (supplemental Methods). Donor blood cell chimerism was determined as indicated. Details are supplied in the supplemental Methods.

Barcoding and barcoding transplant

A 33-bp DNA barcode was generated consisting of a defined 6-bp library sequence at the 5′ (to mark the genotype) followed by a large, random 27-bp (single-cell specific) sequence and cloned into a lentiviral pLKO (GFP) vector. Ckit$^+$ hematopoietic stem and progenitor cells (HSPCs) were isolated from the bone marrow of the different haploinsufficient or compound haploinsufficient mouse lines described herein, cultured for 16 hours before transduction (multiplicity of infection, <0.5). Twenty-four hours after infection, GFP$^+$ cells were sorted and counted manually, and the different genotypes were pooled in equal ratios. Cells (∼500 000 in 150 μL) were injected IV into each of the lethally irradiated mice for the first transplant. Four weeks after transplantation, the excision was induced in the floxed genotypes crossed to *Mx1Cre*$^+$ by poly(IC) injection (supplemental Methods). For the second transplant, 3×10^6 whole bone marrow cells from each mouse were transplanted into lethally irradiated second recipients.

Genomic DNA was isolated from purified cell populations at selected time points. A polymerase chain reaction step was used to amplify the DNA barcode. Sequencing was performed on an Illumina GAII sequencer of the RNAi consortium at the Broad Institute. Details are described in the supplemental Methods.

Single-cell sequencing

Bone marrow was isolated and the lineage depleted by magnetic bead separation with an indirect lineage depletion kit (Milteny Biotec). Lineage-negative (lin$^-$) bone marrow was analyzed, and viable lin$^-$Sca1$^+$ckit$^+$ (LSK) HSC were sorted. Sorted cells were processed using the 10x Genomics Chromium Controller pipeline. Details are supplied in the supplemental Methods.

Dynamical systems model

For each genotype, the dynamic systems model considered mitotic cells in the bone marrow and mature granulocytes in the

bloodstream. Mitotic cells are characterized by their proliferation rate (quantifying the number of divisions per unit of time) and their self-renewal probability (quantifying the probability that progeny of a mitotic cell is mitotic; ie, nonmature). Self-renewal and proliferation are regulated by nonlinear feedback loops. The proliferation rate depends on the number of mature granulocytes. The self-renewal probability in the model depends on the number of mitotic bone marrow cells, which reflects the impact of microenvironmental cues for the regulation of self-renewal. The feedback loops and properties of WT cells are calibrated based on experimental data after bone marrow transplantation. Proliferation and self-renewal of the haploinsufficient genotypes are fitted to the data from the barcoding experiments. A detailed model description is provided in the supplemental Methods.

Quantification and statistical analysis

Statistical analysis, excluding that for single-cell RNA-sequencing data, was conducted with GraphPad Prism v8.0 and v9.0. Unless otherwise specified, data are presented as the mean ± standard error of the mean. *P* values lower than .05 were considered statistically significant. Significance is indicated as follows: $*P \leq .05$; $**P \leq .005$; $***P \leq .0005$; $****P \leq .00005$.

Results

Genetic barcoding in a competitive setting allows for tracking of single clones over time

To dissect the clonal advantage of genetically heterogeneous cells on a single-cell level and their relative contribution to hematopoiesis, a genetic barcoding approach for competitive transplants was established by modifying previously published lentiviral genetic barcoding strategies.[25] This cellular barcoding approach systematically compares genes implicated in the pathogenesis of del(5q) MDS in direct competition with each other and WT cells with single-clone resolution.

HSPCs from heterozygously floxed *Csnk1a1* and *Apc* mice crossed with *Mx1Cre*$^{+}$ mice, from heterozygous *Egr1* mice and *Mx1Cre*$^{+}$ cells, as WT controls were isolated and transduced with a genotype-specific barcode library (Figure 1A; supplemental Figure 2A). Because the object was to analyze the potential for clonal expansion and not engraftment, the excision of the floxed alleles was induced by polyinosinic-polycytidylic acid [poly(I:C)] injection 4 weeks after transplantation (Figure 1A, after engraftment). High gene marking (GFP^{+}) at the end of the first transplant in both hematopoietic progenitor cells and lineages proved that successful long-term reconstitution of hematopoiesis by transplanted barcoded HSPCs was achieved. It reached 95%±4% within the granulocyte compartment at 26 weeks and 83.6%±11% in the LSK compartment at 26 weeks (supplemental Figure 2B). The clonal output within the granulocyte lineage correlated with the clonal proportions in the LSK progenitor cell compartment, as has been reported,[25,26] indicating that the clonal composition of the granulocyte lineage reflects the clonal composition of the stem cell compartment.

Recovered barcodes at the start of the experiment (first time point; week 4, before poly(I:C)) showed engraftment of libraries from all genotypes with high clonal complexity (supplemental Figure 2C-D). WT clones showed the highest "richness," in terms of the highest number of unique clones, followed by *Csnk1a1*, *Egr1*, and *Apc* haploinsufficient clones (supplemental Figure 2D).

Unbiased clustering on barcode composition per time point faithfully grouped samples from the same mouse together, suggesting only minimal barcode sharing (supplemental Figure 3). WT clones showed the highest proportional engraftment on average followed by *Csnk1a1*, *Egr1*, and finally *Apc* haploinsufficient clones (see Figure 3B). Clonal composition of genotypes, as well as expansion of single clones and their contribution to blood lineages, was followed over time. Dominating clones, reconstituting 95% of hematopoiesis, changed greatly within the first 4 weeks, in line with previous reports of barcoded hematopoiesis in a transplantation setting.[27] In our experimental model of competing del(5q) haploinsufficient genes and WT hematopoiesis, the overall number of unique clones reconstituting 95% of granulopoiesis and the diversity of the clonal population decreased steadily over time (supplemental Figure 2C-D).

WT hematopoiesis is recurrently outcompeted by del(5q) genotypes

The LSK fraction in the bone marrow of 5 transplant-recipient mice showed heterogeneous proportions of genotypes among the mice after 26 weeks (Figure 1B). Mouse 2 showed oligoclonal expansion of *Egr1*$^{+/-}$ and *Csnk1a1*$^{+/-}$ clones in the bone marrow in 2 consecutive transplants with nearly complete repression of WT hematopoiesis. In mouse 3, large oligoclonal *Csnk1a1*$^{+/-}$ clones steadily expanded, and 2 distinct clones completely dominated the bone marrow in the second transplant (Figure 1B-C). In both mice, the dominance of *Csnk1a1*$^{+/-}$ clones increased, whereas the number of clones per genotype decreased. WT hematopoiesis was steadily outcompeted in mice 2, 3, and 4 in the first transplant and in mice 1, 2, and 3 in the second transplant (Figure 1B-C; supplemental Figure 2D). These data highlight that the advantage of del(5q) genotypes, compared with WT cells, manifests slowly but steadily, and is enhanced by additional stress (eg, secondary transplantation).

Changes in cell properties can faithfully model clonal evolution of barcoded genotypes

We hypothesized that the heterogeneity of clonal composition among recipient mice could be caused by (1) a varying number of transplanted/engrafted cells per genotype because of stochastic sampling from a limited cell pool, (2) different clonal driver fitness of the transplanted genotypes, and (3) different response to environmental factors. To test these hypotheses and check the validity of the genetic barcoding transplantation experiments, a dynamic systems model was developed based on experimental data (Figure 2A). The model considers 2 compartments: (1) postmitotic differentiated cells in the blood with the ability to feed back to the stem cell compartment and (2) an actively dividing progenitor compartment with different self-renewal and proliferation properties for each genotype (Figure 2A). Proliferation and self-renewal may be different for each genotype. Importantly, experimental data were in agreement with the model 8 to 26 weeks after transplantation (Figure 2D), indicating that the experimental results can be explained by the competition of different genotypes with specific cell properties. The fit of the model implies that *Csnk1a1* haploinsufficient stem cells showed a trend toward decreased proliferation (Figure 2B) but increased self-renewal (Figure 2C) compared with WT (optimal fit of self-renewal larger than self-renewal of WT in all mice ($P < .1$ in 1 mouse; Figure 2C) and a relatively small variation among the mice. The data also indicate that *Csnk1a1* haploinsufficient cells were more robust (eg, to extrinsic conditions), whereas *Egr1*

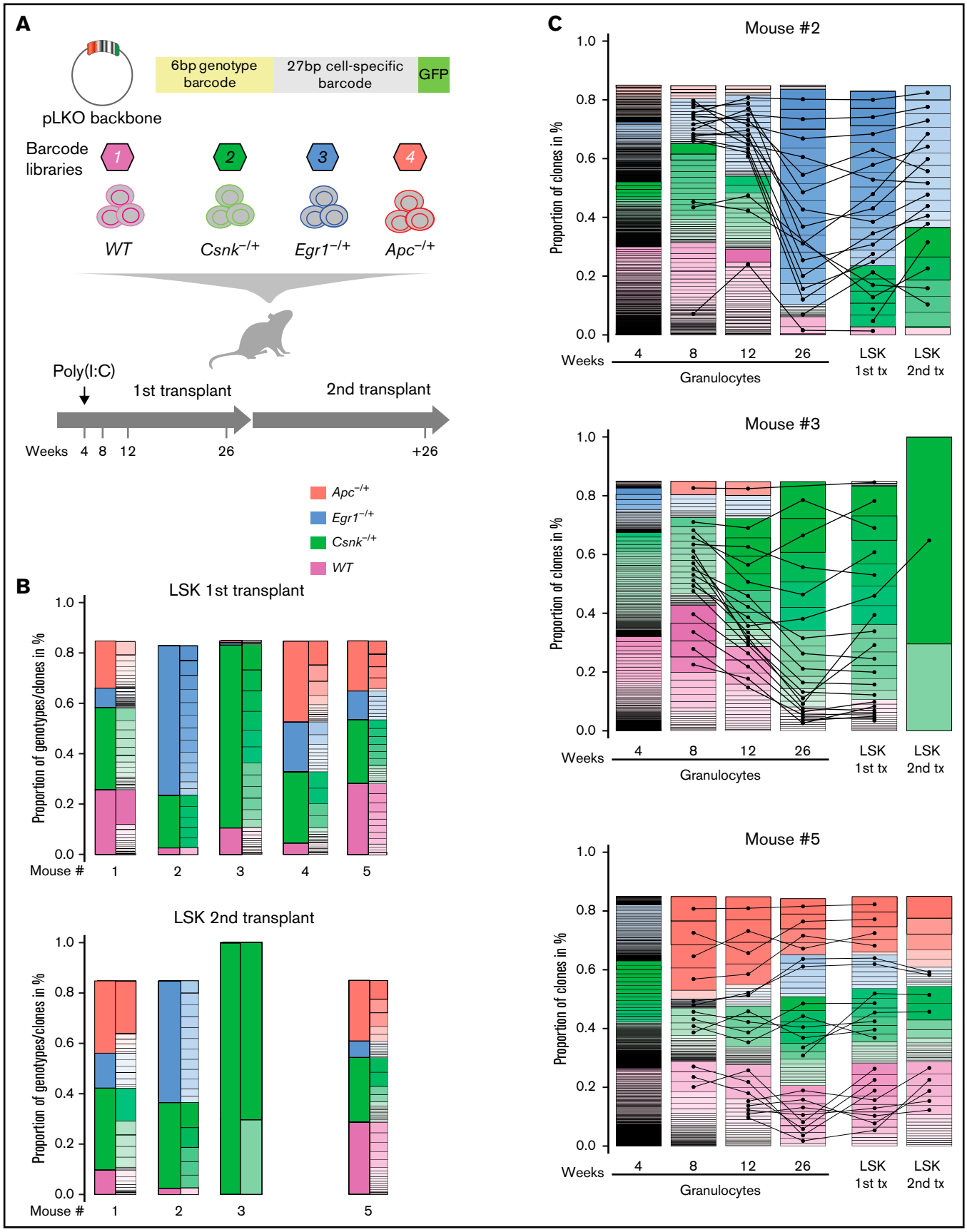
A
6bp genotype barcode
27bp cell-specific barcode
GFP
pLKO backbone
Barcode libraries
1
2
3
4
WT
Csnk−/+
Egr1−/+
Apc−/+
Poly(I:C)
1st transplant
2nd transplant
Weeks 4 8 12 26 +26
Apc−/+
Egr1−/+
Csnk−/+
WT
B
LSK 1st transplant
Proportion of genotypes/clones in %
Mouse # 1 2 3 4 5
LSK 2nd transplant
Proportion of genotypes/clones in %
Mouse # 1 2 3 5
C
Mouse #2
Proportion of clones in %
Weeks 4 8 12 26 LSK 1st tx LSK 2nd tx
Granulocytes
Mouse #3
Proportion of clones in %
Weeks 4 8 12 26 LSK 1st tx LSK 2nd tx
Granulocytes
Mouse #5
Proportion of clones in %
Weeks 4 8 12 26 LSK 1st tx LSK 2nd tx
Granulocytes

Figure 1.

haploinsufficient cells were more variable in regard to self-renewal parameters (Figure 2C). *Apc* haploinsufficient clones interestingly showed a trend toward higher proliferation in some mice that may explain why they are exhausted over time, in line with previous reports.[18] The disagreement between the model and the data at 4 weeks after transplantation could have been caused by temporary engraftment of progenitor cells from the transplant that show stochastic fluctuation and exhaustion over time.[28]

As genotypes in the experiments did not engraft in strictly equal proportions and demonstrated experimental variation (supplemental Figure 1D), computer simulations were run to determine how differences in the number of engrafted cells affect the interindividual heterogeneity of clonal evolution. To take environmental (extrinsic) or individual factors into account, the impact of small variations of cell properties (proliferation and self-renewal) on clonal evolution was also simulated. Perturbing the number of transplanted (or engrafted) cells per genotype (within a ±20% range) barely affected the proportions of competing genotypes (Figure 2E). Notably, perturbation of cell properties within a ±20% range had a strong impact on the expansion of the respective genotype (Figure 2F), which suggests that differences in the number of cells at engraftment play a less significant role in clonal evolution than interindividual differences in cell properties (eg, response to environmental factors and intrinsic differences). Simulations perturbing the initial clone size demonstrates that the number of cells initially engrafted does not impact if a clone expands or decreases (Figure 2G). In contrast, genotype-specific cell parameters strongly determined the expansion capacity of a clone (Figure 2G).

The genotypes *Csnk1a1* and *Egr1* have the potential to clonally expand

The del(5q) genotypes, *Csnk1a1* and *Egr1*, started steady (oligo)clonal expansion, whereas most *Apc* clones were exhausted over time or were effectively outcompeted (Figures 1C and 2B; supplemental Figure 2D). Because completely equal engraftment of genotypes among mice was not observed, genotype-specific growth dynamics, independent of the total abundance or clone size of a genotype across mice, was tested throughout all time points after the first transplant. Initially, clones from all mice were pooled and then normalized to their size at week 8. The individual clones per genotype were then categorized into (1) expanding (doubling), (2) steady, and (3) decreasing. A significantly larger fraction of expanding *Csnk1a1* and *Egr1* haploinsufficient clones compared with WT clones (Figure 3A) was found, suggesting increased expansion behavior and stability of clones from these genotypes, regardless of the total clone size.

To test genotype expansion independent of the abundance at engraftment, genotype abundance throughout first and second transplant was examined. A significant proportional increase in clones with *Csnk1a1* haploinsufficiency from week 8 in granulocytes to week 26 of the first transplant and throughout 26 weeks of the secondary transplant in HSCs (LSK; Figure 3B) was noted. This demonstrates that *Csnk1a1* and *Egr1* haploinsufficient HSCs have the potential to clonally expand and to dominate hematopoiesis, despite their heterogeneity at engraftment and despite differences in microenvironmental cues. *Csnk1a1* haploinsufficient clones showed an increased competitive advantage by steadily increasing in proportion through the first and second transplant. In particular *Apc* haploinsufficient clones engrafted poorly but proliferated and persist (Figure 2).

In summary, we demonstrated that genetic haploinsufficiency of del(5q) genes can lead to an oligoclonal expansion of HSCs, which was assumed but had not been shown formally. Clonal expansion slowly but steadily progresses and is enhanced by secondary transplantation, leading to clone selection.

Csnk1a1 haploinsufficiency alone clonally dominates the bone marrow, in comparison with combinations with *Apc* and *Egr1*, and is dependent on β-catenin

How combined haploinsufficient clones would behave within 1 microenvironment was then examined. Based on our data, we had hypothesized that nuclear induction of β-catenin in *Csnk1a1* haploinsufficiency is a major driver of HSC expansion.[1] To functionally test that the proliferative advantage of *Csnk1a1* haploinsufficiency is abolished when β-catenin expression is decreased (β-catenin haploinsufficiency), we included $Csnk1a1^{+/-}Ctnnb1^{+/-}Mx1Cre^{+}$ cells in the systematic comparison. In this approach, barcoded ckit^{+} cells isolated from (1) $Mx1Cre^{+}$ as WT, (2) $Csnk1a1^{+/fl}Apc^{+/fl}Mx1Cre^{+}$, (3) $Csnk1a1^{+/fl}Egr1^{+/-}Mx1Cre^{+}$, (4) $Csnk1a1^{+/fl}$Mx1Cre^{+}, and (5) $Csnk1a1^{+/fl}Ctnnb1^{+/-}Mx1Cre^{+}$ mice were transplanted. Again, barcode marking was high, and WT clones showed the highest mean proportional engraftment after 4 weeks in the granulocyte compartment (34.2% ± 16.4%) followed by *Csnk1a1* haploinsufficient clones (26.8% ± 6.8%), *Csnk1a1/Egr1* haploinsufficient clones (22.9% ± 18.8%), *Csnk1a1/Ctnnb1* haploinsufficient clones (16% ± 6.7%), and *Csnk1a1/Apc* haploinsufficient clones (9.9% ± 2%; Figure 4C; supplemental Figure 4A). Clustering on the Morisita-Horn index of barcodes per time point grouped samples from the same mouse together (supplemental Figure 4D).

The clonal composition of the bone marrow in first and second transplants (Figure 4A) was then analyzed. *Csnk1a1* haploinsufficient LSK cells dominated the bone marrow over combined haploinsufficiency of *Egr1* and *Apc* and expanded (oligo)clonally, in particular in the second transplant (Figure 4A-B). As also seen in the conventional competitive transplantation assay (see Figure 5), $Csnk1a1^{+/-}Apc^{+/-}$ and $Csnk1a1^{+/-}Ctnnb1^{+/-}$ LSK cells were outcompeted in the HSC fraction and performed even worse than WT cells, indicating that too high and too low levels of β-catenin are detrimental to HSC function. Again, a significant increase in the proportion of clones was seen with *Csnk1a1* haploinsufficiency starting at week 4 in the peripheral blood and throughout the HSC analysis in the bone marrow in the first

Figure 1. Genetic barcoding in a competitive setting allows for the tracking of single clones over time. (A) Experimental design. HSPCs of different del(5q) genotypes were transduced with a lentiviral vector containing synthesized genetic barcodes, sort purified for GFP expression, mixed, and transplanted in an equal ratio into WT recipients (n = 5). (B) Genotype composition of 85% dominant barcoded clones within the bone marrow LSK fraction after the first and second transplants. The right half of the stacked bars represents individual clones. Mouse 4 died after the first transplant. (C) Representative example of the 85% dominant clones within granulocytes and LSK cells over time in mice 2, 3, and 5. Lines represent the tracking of the 20 largest LSK clones (first transplant) throughout the other time points.

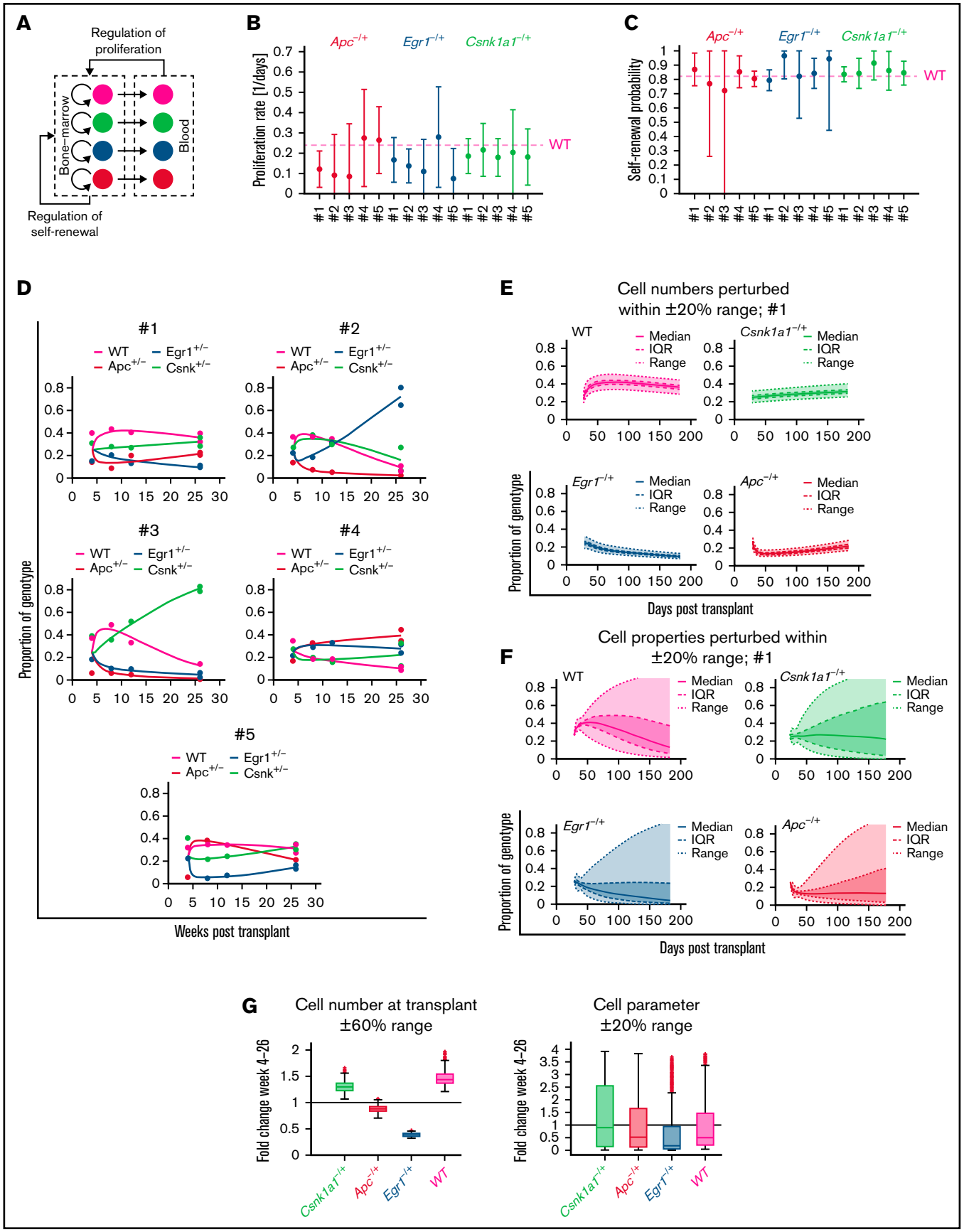
A
Regulation of proliferation
Bone-marrow
Blood
Regulation of self-renewal
B
Apc−/+
Egr1−/+
Csnk1a1−/+
Proliferation rate [1/days]
WT
C
Self-renewal probability
D
#1
#2
#3
#4
#5
WT
Apc+/−
Egr1+/−
Csnk+/−
Proportion of genotype
Weeks post transplant
E
Cell numbers perturbed within ±20% range; #1
Median
IQR
Range
Days post transplant
F
Cell properties perturbed within ±20% range; #1
G
Cell number at transplant ±60% range
Cell parameter ±20% range
Fold change week 4–26

Figure 2.

and second transplant (Figure 4C). All other genotypes including WT cells were outcompeted (Figure 4C).

Csnk1a1 or *Egr1* haploinsufficiency alone has a stronger competitive advantage than combinations of *Csnk1a1* with *Apc* and *Egr1* haploinsufficiency

To validate the findings from the competitive genetic barcoding experiments, the same genotypes were tested in conventional competitive transplants, where genes of interest compete with WT competitor cells. Comparable to the genetic barcoding approach, mouse models with haploinsufficiency for *Csnk1a1*, *Apc*, *Egr1*, and *Ctnnb1*, as well as double-haploinsufficient mice, to test a combinatorial effect (Figure 5A), were included. Equal engraftment of all genotypes at 4 and 8 weeks after transplant (before and after poly(I:C) induction) was observed, confirming that there is no engraftment deficit for any of the tested genotypes (supplemental Figure 5A). Furthermore, no major changes in the proportions within the LSK compartment, when CD45.2 (haploinsufficient genotypes) were compared to the CD45.1 WT competitor cells (supplemental Figure 5C), were detected.

Over time, *Csnk1a1* haploinsufficient HSCs gained an advantage over WT cells in the blood during the first transplant. This advantage was reestablished in the secondary transplant, where *Egr1* haploinsufficient cells also outcompeted WT cells in the blood over time (Figure 5B). Both *Csnk1a1* and *Egr1* haploinsufficiency alone, as well as the combined haploinsufficiency of *Csnk1a1* and *Egr1*, led to a significant dominance of CD45.2$^+$ LSKs in the bone marrow at the end of the secondary transplant. *Apc* haploinsufficient LSKs did not outcompete WT LSKs in the first transplant and were depleted in the secondary transplant (Figure 5C). This is in accordance to previously published data of reduced long-term repopulation capacity of *Apc* haploinsufficient HSCs.[8,18]

The combination of *Csnk1a1/Egr1* haploinsufficiency gained an advantage over WT LSKs only in the secondary transplant. Interestingly, the combination of *Csnk1a1/Apc* and *Csnk1a1/Ctnnb1* haploinsufficiency was comparable to WT LSKs. *Ctnnb1* haploinsufficiency alone led to a significant disadvantage of the HSC function, as seen within LSK bone marrow and blood cell output in the first transplant and more pronounced in the secondary transplant (Figure 5B-C). β-Catenin protein levels measured by intracellular flow cytometry were graded in LSKs from WT, *Csnk1a1*$^{-/+}$, *Csnk1a1*$^{-/+}$*Apc*$^{-/+}$, and *Csnk1a1*$^{-/+}$*Ctnnb1*$^{/+}$ mice. They were elevated in *Csnk1a1*$^{-/+}$ LSK, highest in *Csnk1a1*$^{-/+}$*Apc*$^{-/+}$LSK, and comparable to WT in *Csnk1a1*$^{-/+}$*Ctnnb1*$^{/+}$ LSK (supplemental Figure 5B). This highlights the sensitivity of HSCs to β-catenin dosage in regard to their competitive performance.[29]

The systematic comparison of different haploinsufficient del(5q) MDS genes in the gold standard of competitive transplantation thus recapitulated the findings from the genetic barcoding competitive transplants. It was shown that *Csnk1a1* and *Egr1* haploinsufficient cells outcompete WT competitor cells over time in a secondary transplant and suggest that *Csnk1a1* and *Egr1* particularly contribute to the clonal advantage of the HSC in del(5q) MDS. The results did not confirm our initial hypothesis of combinatorial effects of *Csnk1a1* and *Egr1* haploinsufficiency, leading to a more pronounced clonal expansion.

Csnk1a1 haploinsufficient HSCs show proproliferative signaling and metabolic activation

How *Csnk1a1* haploinsufficiency leads to steady clonal expansion, while increasing (or maintaining) stem cell fitness over successive transplantation was investigated next. To evaluate the cell intrinsic differences between *Csnk1a1* haploinsufficient HSCs and WT (*Mx1Cre*$^+$) HSCs, single-cell RNA-sequencing of the progenitor compartment was performed 24 weeks after transplantation into WT recipients comparable to the competitive assays (*Csnk1a1*$^{-/+}$*Mx1Cre*$^+$ [6 mice, ~33 000 single cells; WT/*Mx1Cre*$^+$ (5 mice], ~42 000 cells; supplemental Figure 6A-D). Downregulation of *Csnk1a1* in the haploinsufficient condition could be confirmed in all cell clusters (supplemental Figure 6E).

Unsupervised clustering of recovered cells led to the identification of 12 clusters (Figure 6A; supplemental Figure 6F). These 12 identified clusters formed a continuum of differentiation and cell cycle activation from naive and quiescent hematopoietic stem cells to

Figure 2. Perturbation of cell properties can faithfully model clonal evolution of barcoded genotypes. (A) Structure of the mathematical model. The model considers proliferation and self-renewal of mitotic cells in the bone marrow that give rise to circulating granulocytes. For simplicity, the mitotic cell types are modeled as 1 cell population. Mitotic cells are characterized by their kinetic cell properties: proliferation rate (quantifying the number of divisions per unit of time) and self-renewal probability (the probability that offspring originating from division are again mitotic cells). In agreement with the data, proliferation and self-renewal are regulated by feedback loops depending on the number of mature and mitotic cells, respectively. The model takes into account 4 different genotypes (WT, *Apc*$^{+/-}$, *Egr1*$^{+/-}$, and *Csnk1a1*$^{+/-}$) with different cell properties. (B-C) The fitted proliferation rates (B) and self-renewal probabilities (C) per mouse for *Apc*$^{+/-}$, *Egr1*$^{+/-}$, and *Csnk*$^{+/-}$ mice (1-5) with the respective 95% confidence intervals. The WT cell properties are indicated with a pink dotted line. (D) Fit of the model to the 5 mice. Cell properties (proliferation rates and self-renewal probabilities) of WT cells have been calibrated based on steady cell counts and reconstitution after bone marrow transplantation. Cell properties of other genotypes have been fitted to the data. The measured cell counts of each of the genotypes have been pooled. Dots signify the experimental data points; lines signify the model predictions. (E) Trajectories of clonal evolution are robust with respect to perturbations of the initial number of cells. The depicted simulations show how the clonal evolution in mouse 1 depends on the number of initial cells. The number of cells of each genotype had been independently perturbed in the range of ±20%. The differences in the initial number of cells between the genotypes resulted only in minor changes in the observed clonal evolution. The figure is based on 1000 simulations, with random perturbations from a uniform distribution. (F) Trajectories of clonal evolution are sensitive to small changes in mitotic cell properties (proliferation rates and self-renewal probabilities). The depicted simulations show how the clonal evolution in mouse 1 changed if proliferation and self-renewal of *Apc*$^{+/-}$, *Egr1*$^{+/-}$, and *Csnk1a1*$^{+/-}$cells were perturbed by ±20%. The figure is based on 1000 simulations, with randomly perturbed cell properties from a uniform distribution. (G) Fold change in the number of cells between weeks 4 and 26 is robust with respect to perturbations of the initial cell number but sensitive to small changes in mitotic cell properties. The panels show the fold change in the number of cells for each genotype in mouse 1 for perturbed initial cell counts (top) and perturbed mitotic cell properties (ie, proliferation rates and self-renewal probabilities of *Apc*$^{+/-}$, *Egr1*$^{+/-}$, and *Csnk1a1*$^{+/-}$cells; bottom). The initial number of cells was independently perturbed in the range of ±60%. Cell properties were perturbed in the range of ±20%. The figure is based on 1000 simulations. Perturbations were sampled from a uniform distribution.

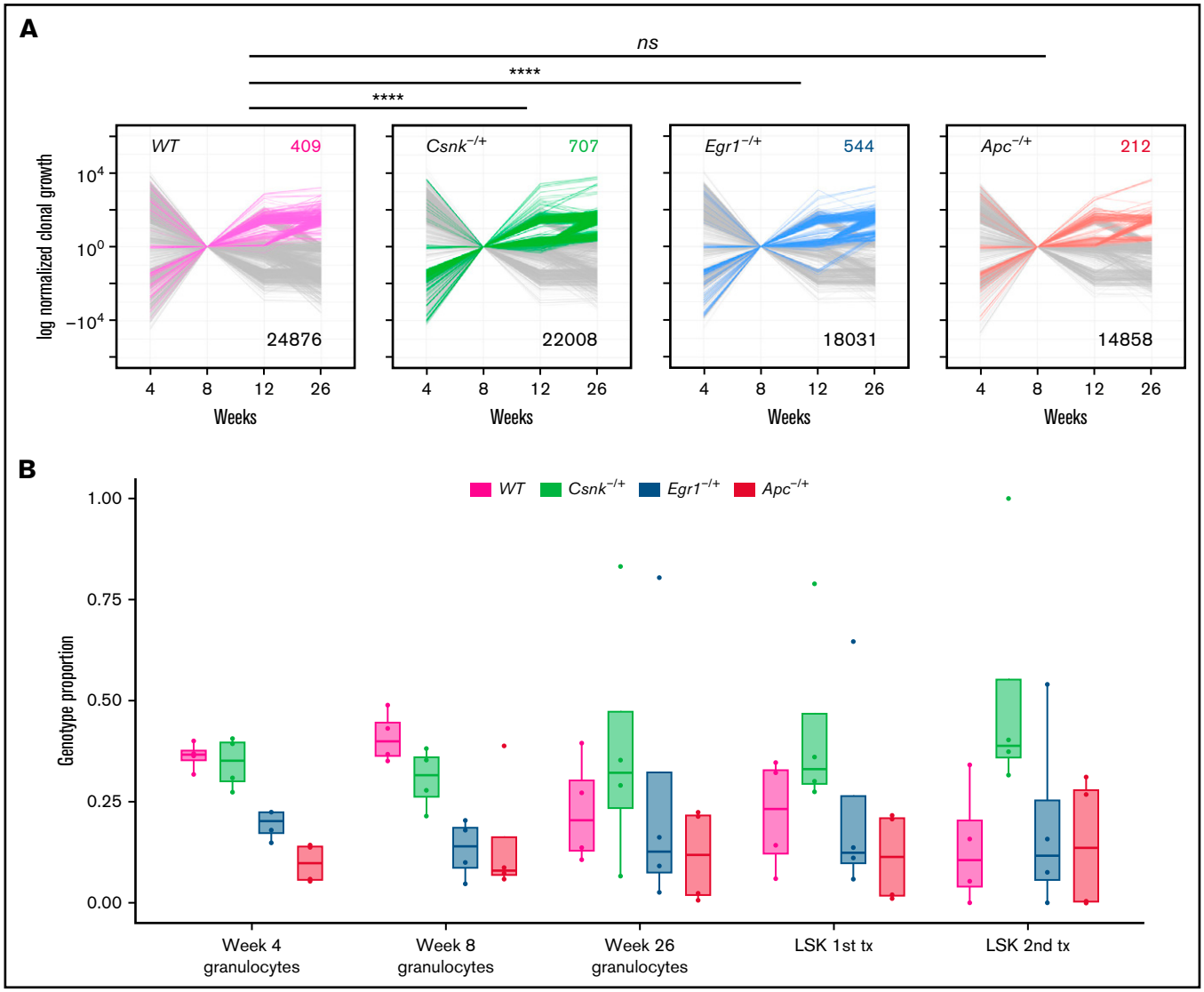

Figure 3. The del(5q) genotypes *Csnk1a1* and *Egr1* have the potential to expand clonally. (A) Clonal growth over time, separated per genotype. Only the larger clones summing up to 99% cumulative abundance are considered. Clonal growth is obtained by the ratio between the proportion of a given clone divided by its proportion at week 8. A pseudocount of 1 is added to all clones to estimate proportions. Colored lines represent expanded clones (log-ratio ≥1 at week 26). Pearson's χ^2 test with Yates continuity correction was applied to test for independence between clonal expansion and genotype (WT-*Csnk1a1*; P = 8.214970e-27; WT-*Egr1*; P = 2.721056e-20; WT-*Apc*; P = .1047533; P-values adjusted with the Benjamini-Hochberg procedure). ****P < .00001. (B) Comparison of genotype abundance, across the 4 mice, at weeks 4, 8, and 26 (granulocytes); week 26 (LSK); and week 52 (LSK) after the second transplant. Only the larger clones summing to 99% cumulative abundance were considered. The Page test for monotonically increasing ranks was applied to the time points at weeks 8, 26, and 52 for each of the 4 genotypes, with only *Csnk1a1* rejecting the null hypothesis of abundances being equal over time (P = .00666). Data are represented as boxplots; boxes include Q_1 to Q_3, with the median indicated. Tx, transplant.

lineage marker–expressing, highly cell cycle–active, committed progenitors. All cell clusters were represented in both *Csnk1a1* haploinsufficient and WT cells (Figure 6B). The most immature HSC cluster was reduced in the *Csnk1a1* condition compared with WT, whereas the downstream uncommitted progenitors (ST-HSC, intermediate progenitors, such as MPP2-3) were expanded (supplemental Figure 6C-D).

Gene set enrichment analysis of hallmark gene sets within each population was performed to compare *Csnk1a1* haploinsufficient cells and WT cells. Significant upregulation of proliferative and differentiation pathways, such as the hallmark pathways Myc targets, E2F targets, and oxidative phosphorylation, were observed. These pathways were significantly upregulated in *Csnk1a1* haploinsufficient cells in the LT-HSC cluster as well as ST-HSC, megakaryocyte/erythroid progenitors, and early MPP clusters. In more committed progenitor clusters, such as myeloid progenitors (Figure 6C), this upregulation was not apparent. Upregulation of downstream target genes of the transcription factors Myc and E2f suggests active proliferation and differentiation of haploinsufficient *Csnk1a1* cells.[30] This result is in line with finding S-phase–related genes upregulated in the haploinsufficient samples (Figure 6D),

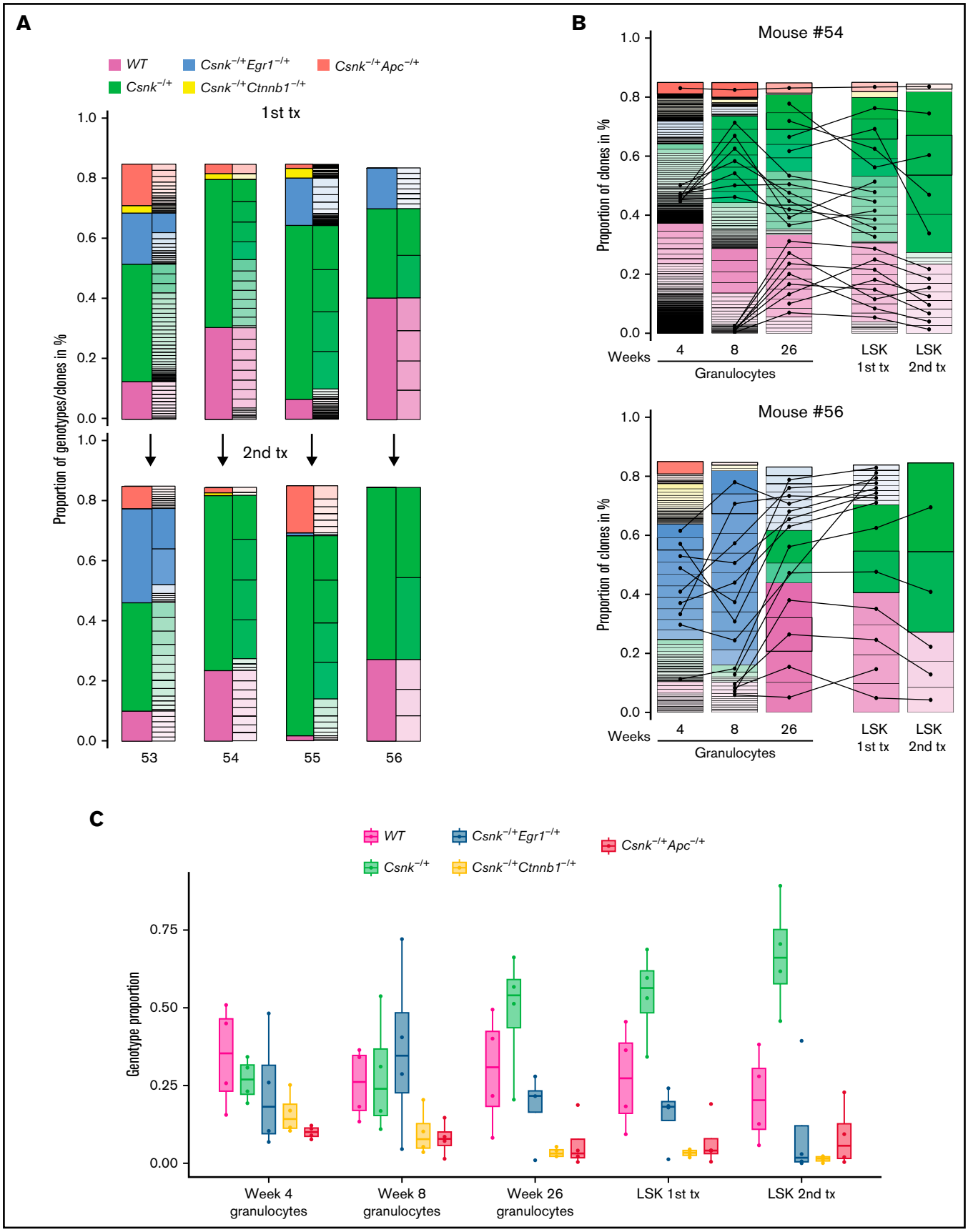
A
WT
Csnk−/+
Csnk−/+Egr1−/+
Csnk−/+Ctnnb1−/+
Csnk−/+Apc−/+
1st tx
2nd tx
Proportion of genotypes/clones in %
1.0
0.8
0.6
0.4
0.2
0.0
53
54
55
56
B
Mouse #54
Mouse #56
Proportion of clones in %
Weeks
4
8
26
Granulocytes
LSK
1st tx
LSK
2nd tx
C
Genotype proportion
0.75
0.50
0.25
0.00
Week 4
granulocytes
Week 8
granulocytes
Week 26
granulocytes
LSK 1st tx
LSK 2nd tx

Figure 4.

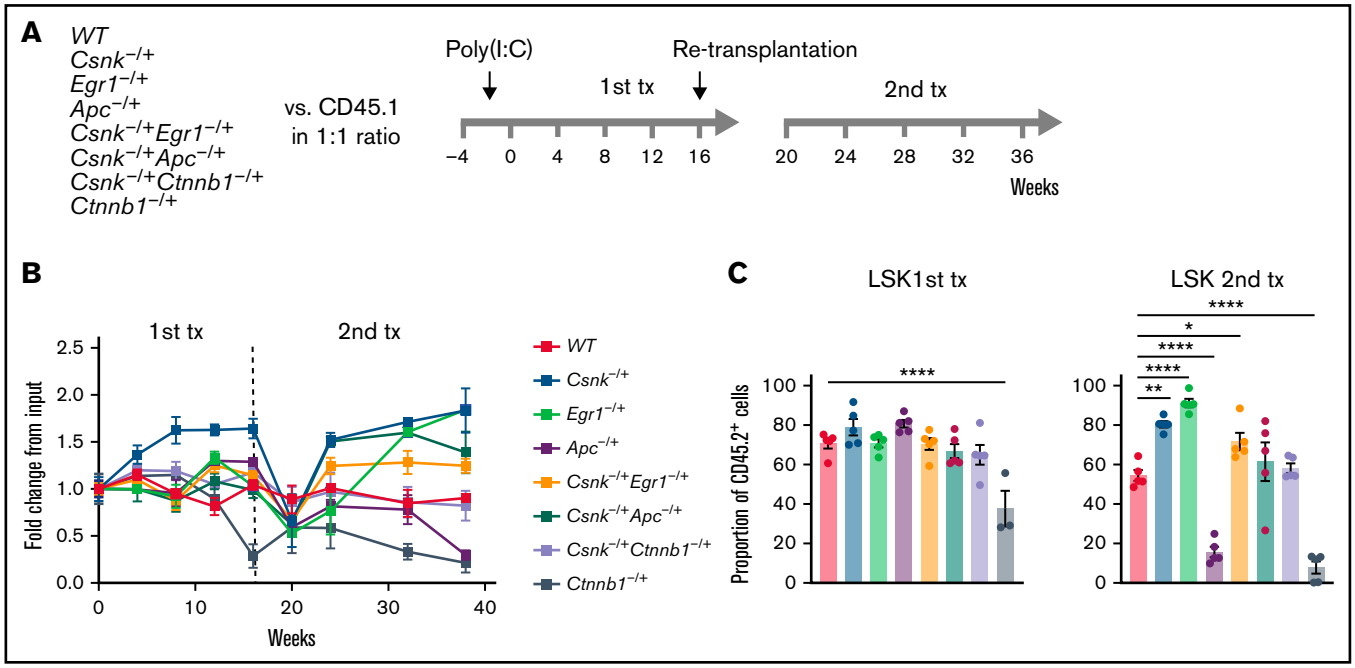

Figure 5. *Csnk1a1* or *Egr1* haploinsufficiency alone has a stronger competitive advantage than combinations of *Csnk1a1* with *Apc* and *Egr1* haploinsufficiency. (A) Experimental design. Competitive transplantation of ckit$^+$ HSPCs from *Mx1-Cre*$^+$ (WT), *Csnk1a1*$^{fl/+}$*Mx1-Cre*$^+$ (*Csnk*$^{-/+}$), *Apc*$^{fl/+}$ *Mx1-Cre*$^+$ (*Apc*$^{-/+}$), and *Egr1*$^{+/-}$(*Egr1*$^{-/+}$), *Csnk1a1*$^{fl/+}$*Egr1*$^{-/+}$*Mx1Cre*$^+$ (*Csnk*$^{-/+}$*Egr1*$^{-/+}$), *Csnk1a1*$^{fl/+}$*Apc*$^{fl/+}$*Mx1Cre*$^+$ (*Csnk*$^{-/+}$*Apc*$^{-/+}$), *Csnk1a1*$^{fl/+}$*Ctnnb1*$^{fl/+}$*Mx1Cre*$^+$ (*Csnk*$^{-/+}$*Ctnnb1*$^{-/+}$), *Ctnnb1*$^{fl/+}$*Mx1Cre*$^+$ (*Ctnnb1*$^{-/+}$) mixed 1:1 with CD45.1$^+$ ckit$^+$ WT competitor cells (n = 5 each). (B) Fold change in 45.2$^+$ cells in the peripheral blood of recipients relative to input during the first and second transplants. Data are represented as the mean ± standard error of the mean (SEM). (C) Percentage of CD45.2$^+$ cells in the bone marrow LSK (lin$^-$;Sca1$^+$;ckit$^+$) after the first and second transplants. Statistical significance tested by 1-way analysis of variance with Dunnett's multiple-comparison test. Data are represented as the mean ± SEM. *$P \leq .05$; **$P \leq .005$; ****$P \leq .00005$.Tx, transplant.

corroborating previous findings of increased cell cycle activity in *Csnk1a1* haploinsufficient LSK with flow cytometry.[1]

Downregulation of inflammatory pathways in *Csnk1a1* haploinsufficient HSCs

Simultaneously, and unexpectedly, significant downregulation was observed in pathways related to inflammatory signaling, such as TNF-α signaling via NF-κB and interferon-α response (Figure 6C,E-F). These changes were mostly seen in immature populations and were especially pronounced in LT-HSCs and ST-HSCs, as well as in erythroid/megakaryocytic lineage progenitors (Figure 6E- F). Predictions of transcription factor activity by testing enrichment of transcriptional target gene regulons fit well with this assumption by predicting increased activity of well-known drivers of proliferation and differentiation. These include the transcription factors *Myc* and *Myb* in LT-HSCs with concurrent decrease of *Stat1*, *Stat3*, *Irf1* (interferon-α response) and *Rela* (NF-κB) activity (Figure 6G). Differential gene expression comparing *Csnk1a1* haploinsufficient cells to WT cells in the different HSC clusters was used to infer pathway activity based on pathway perturbation footprint data.[31] In line with the findings from the gene set enrichment analysis, the pathways JAK-STAT, TNF-α, and NF-κB signaling were downregulated and most pronounced in LT-HSC and erythroid progenitors (supplemental Figure 6G).

We hypothesized that downregulation of inflammatory signaling in the most immature hematopoietic stem cells may confer a competitive advantage to *Csnk1a1* haploinsufficient HSCs that is exacerbated in stress conditions such as inflammatory stress and serial transplantation. Therefore, the performance of *Csnk1a1* haploinsufficient stem cells under exogenous inflammatory stress was tested.

The competitive advantage of *Csnk1a1* haploinsufficient HSCs is increased under exogenous inflammatory stress

The function of *Csnk1a1* haploinsufficient and WT HSCs under exogenous inflammatory stress in vivo in a competitive transplantation assay was tested. Because TNF-α and IFN signaling was

Figure 4. *Csnk1a1* alone clonally dominates the bone marrow in comparison with combinations with *Apc* and *Egr1* and is dependent on β-catenin. (A) Genotype composition of 85% dominant barcoded clones within the bone marrow in the LSK fraction after the first and second transplants. (B) Representative example of 85% dominant clonal proportions within granulocytes and LSK cells over time in mice 54 and 56. Lines represent the tracking of the 20 largest clones in LSK cells in the first transplant throughout the other time points. (C) Comparison of genotype abundance, across the 4 mice, at weeks 4, 8, and 26 (granulocytes); week 26 (LSK); and week 52 (LSK) after the second transplant. Only the larger clones summing up to 99% cumulative abundance are considered. The Page test for monotonically increasing ranks was applied to time points week 8, 26, and 52 for each of the 4 genotypes, with only *Csnk1a1* rejecting the null hypothesis of abundances being equal over time ($P = .00666$). Data are represented as box plots; boxes include Q_1 to Q_3, with the median indicated. Tx, transplant.

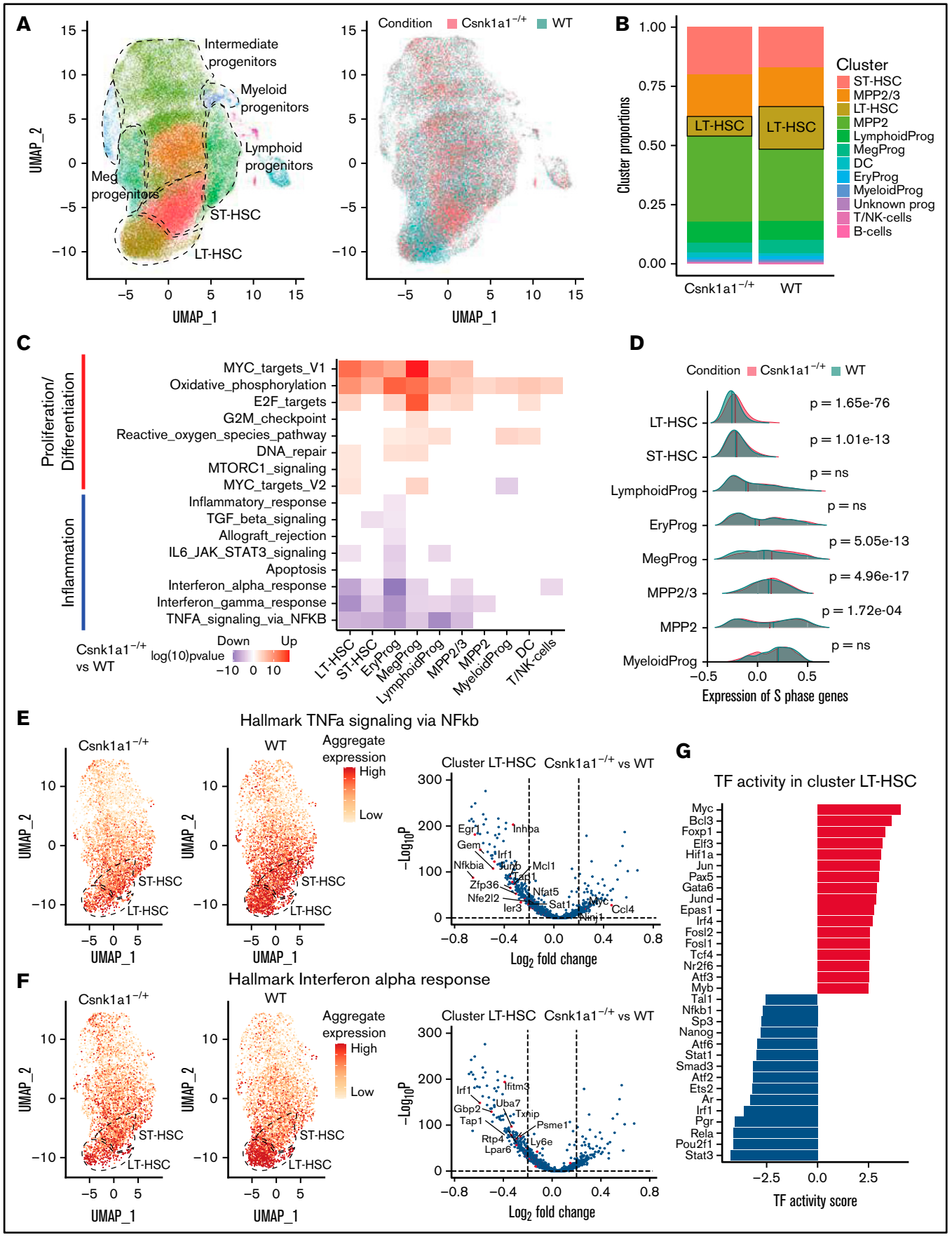
A
Intermediate progenitors
Myeloid progenitors
Lymphoid progenitors
Meg progenitors
ST-HSC
LT-HSC
UMAP_1
UMAP_2
Condition Csnk1a1−/+ WT
B
Cluster proportions
LT-HSC
LT-HSC
Cluster
ST-HSC
MPP2/3
LT-HSC
MPP2
LymphoidProg
MegProg
DC
EryProg
MyeloidProg
Unknown prog
T/NK-cells
B-cells
Csnk1a1−/+
WT
C
Proliferation/ Differentiation
Inflammation
MYC_targets_V1
Oxidative_phosphorylation
E2F_targets
G2M_checkpoint
Reactive_oxygen_species_pathway
DNA_repair
MTORC1_signaling
MYC_targets_V2
Inflammatory_response
TGF_beta_signaling
Allograft_rejection
IL6_JAK_STAT3_signaling
Apoptosis
Interferon_alpha_response
Interferon_gamma_response
TNFA_signaling_via_NFKB
Csnk1a1−/+ vs WT
log(10)pvalue
Down Up
LT-HSC ST-HSC EryProg MegProg LymphoidProg MPP2/3 MPP2 MyeloidProg DC T/NK-cells
D
Condition Csnk1a1−/+ WT
LT-HSC p = 1.65e-76
ST-HSC p = 1.01e-13
LymphoidProg p = ns
EryProg p = ns
MegProg p = 5.05e-13
MPP2/3 p = 4.96e-17
MPP2 p = 1.72e-04
MyeloidProg p = ns
Expression of S phase genes
E
Hallmark TNFa signaling via NFkb
Csnk1a1−/+
WT
Aggregate expression
High
Low
Cluster LT-HSC Csnk1a1−/+ vs WT
−Log10P
Log2 fold change
Egr1
Inhba
Gem
Irf1
Nfkbia
Junb
Mcl1
Tagln
Zfp36
Nfe2l2
Nfat5
Ier3
Sat1
Myc
Ccl4
F
Hallmark Interferon alpha response
Irf1
Ifitm3
Uba7
Gbp2
Txnip
Tap1
Psme1
Rtp4
Ly6e
Lpar6
G
TF activity in cluster LT-HSC
Myc
Bcl3
Foxp1
Elf3
Hif1a
Jun
Pax5
Gata6
Jund
Epas1
Irf4
Fosl2
Fosl1
Tcf4
Nr2f6
Atf3
Myb
Tal1
Nfkb1
Sp3
Nanog
Atf6
Stat1
Smad3
Atf2
Ets2
Ar
Irf1
Pgr
Rela
Pou2f1
Stat3
TF activity score

Figure 6.

particularly affected by *Csnk1a1* haploinsufficiency in the most primitive HSCs, we decided to use poly(I:C) to induce a type 1 interferon response and induction of TNF-α. The effect of poly(I:C) on HSCs is well studied, and it has been shown that it drives HSCs into cycling, ultimately exhausting them.[32-34] In addition, it has been shown that the neighboring genes of *Csnk1a1* on the 5q arm have the potential to induce inflammatory stimuli in the hematopoietic system and the bone marrow niche.[19-21,35]

To test the HSC function of *Csnk1a1* haploinsufficient HSCs in direct competition with WT cells under exogenous, inflammatory stress, transplant-recipient mice were repetitively treated with poly(I:C), starting 4 weeks after transplantation (Figure 7A). *Csnk1a1*$^{-/+}$ myeloid (CD11b^{+}) cells expanded significantly in the peripheral blood when treated with poly(I:C), compared with treatment with phosphate-buffered saline and with stimulated and unstimulated WT cells (Figure 7B). As expected, over the course of the experiment, inflammatory stimulation compromised erythropoiesis more than leukocyte and platelet production, as shown by decreasing peripheral blood hemoglobin values in the poly(I:C) treated groups (Figure 7C; supplemental Figure 7A). *Csnk1a1*$^{-/+}$/WT chimeras showed faster recovery of erythropoiesis after the last (poly(I:C)) stimulus than *Mx1Cre*$^{+}$/WT chimeric mice (Figure 7C). A steady increase of *Csnk1a1*$^{-/+}$ cells was seen, also independent of the inflammatory stimulation over time, suggesting that factors independent of inflammatory stress contribute to the advantage of *Csnk1a1* haploinsufficient cells. In the bone marrow, *Csnk1a1* haploinsufficient cells under inflammatory stress expanded most significantly compared with their WT counterparts, under both stimulated and unstimulated conditions in the CD11b^{+} (myeloid) compartment (Figure 7D). The chimerism of *Csnk1a1* haploinsufficient cells was higher in the stimulated group than in the nonstimulated group, indicating that *Csnk1a1* haploinsufficient cells have an intrinsic clonal advantage that is exaggerated by inflammatory stress. Accordingly, *Csnk1a1* haploinsufficient LSK cells showed higher chimerism in the control setting than their WT counterparts showed, which was even further increased by inflammatory stimulation (Figure 7E). The effect of inflammatory stimulation on *Csnk1a1* expansion was most pronounced in the MPP compartment, but less obvious with LT-HSC (Figure 7E).

These findings prompted a closer look into changes in the frequencies of the HSC compartment of the donor CD45.2 bone marrow after chronic inflammatory exposure. Importantly, only WT LT-HSCs (and CD34^{-} HSCs) treated with poly(I:C) expanded, but not *Csnk1a1* haploinsufficient LT-HSCs in the inflammation-treated groups (Figure 7F). This result is particularly interesting in light of well-studied changes in inflammatory stress and aging that have associated expansion of the CD34^{-} HSC subset with a relative decrease in repopulation capability.[34,36] It also indicates that *Csnk1a1* haploinsufficient LT-HSCs react less to inflammatory stress. This finding agrees with the numerical changes found in the single-cell dataset (compare with Figure 6B; supplemental Figure 6C). Expression of the cell-cycle gene Ki67 was upregulated in *Csnk1a1* haploinsufficient LT-HSCs of treated and untreated mouse cells (Figure 7G), in concordance with previous findings.[1] Cell cycle analysis showed a trend toward increased cell cycle activation in *Csnk1a1* haploinsufficient HSCs treated with poly(I:C). This activation, however, was not significant (supplemental Figure 7B).

In summary, exogenous inflammatory stress increased the competitive advantage of *Csnk1a1* haploinsufficient HSCs. It was accompanied by increased chimerism in the myeloid output of the peripheral blood, as well as bone marrow myeloid cells and in HSCs (LSKs) and was most pronounced in the intermediate progenitors (MPP). WT cells reacted to the inflammatory stimulus with an expansion of (CD34^{-}) LT-HSCs, whereas *Csnk1a1* haploinsufficient CD34^{-} LT-HSCs did not change, suggesting a resistance to inflammation induced remodeling of this compartment.

Discussion

We investigated the relative contribution to the HSC pool of haploinsufficient genes commonly deleted in del(5q) MDS (*Apc*, *Csnk1a1*, and *Egr1*). This was performed in direct competition in 1 mouse and in codeletion, using a genetic barcoding approach and validated by a classic competitive transplantation assay. This approach led to the following observations on the effect of genetic haploinsufficiency on a clonal level: (1) *Csnk1a1* haploinsufficiency provides the greatest clonal advantage of all candidate genes tested; (2) combined *Csnk1a1*/*Egr1* haploinsufficiency does not contribute to further clonal expansion; (3) *Csnk1a1*$^{+/-}$*Apc*$^{+/-}$ and

Figure 6. Downregulation of inflammatory pathways in *Csnk1a1* haploinsufficient HSCs. (A) Uniform Manifold Approximation and Projection (UMAP) visualization of unsupervised clustering of recovered cells (n = 76.963 cells; *Csnk1a1*$^{-/+}$ = 34 578; WT = 42 385). Dashed lines mark populations of interest. (Marker genes per cluster are listed in supplemental Table 3. Cluster identities were identified based on marker genes and transcriptomic similarity to highly sort-purified stem cell populations on the Immunological Genome Project database.) (B) Relative cell proportions per experimental condition color coded by identity cluster, as identified by unsupervised clustering (see supplemental Figure 5C for the fold change of cluster proportions per condition and significance testing) (C) Competitive gene set enrichment analysis (GSEA) using the Camera R package comparing *Csnk1a1*$^{-/+}$ with WT. Filtered for gene sets significantly deregulated with false-discovery rate (FDR) < 0.05 depicted in the heat map: significantly upregulated gene sets in *Csnk1a1*$^{-/+}$ HSCs (red) and downregulated gene sets (blue), with the intensity of the color corresponding to −log(10) of the *P*-value. (D) Density ridge plot of expression of S-phase–related genes per cluster and condition based on Tirosh et al. Means of S-phase gene expression were compared by using Wilcoxon signed-rank test. (E) UMAP visualization of clustered cells featuring aggregated gene set expression of the hallmark gene set TNF-α signaling via NF-κB split by condition (Camera GSEA: LT-HSC cluster *P* = 1.46e-03, ST-HSC cluster *P* = 6.60e-07). Volcano plot showing differentially expressed genes in cluster LT-HSC testing *Csnk1a1*$^{-/+}$ vs WT with genes belonging to hallmark pathway TNF-α signaling via NF-κB highlighted in red and labeled with gene name (right). Positive log2FC, overexpressed *Csnk1a1*$^{-/+}$; negative log2FC, downregulated in Csnk1a1$^{-/+}$. (Differentially expressed genes between conditions per cluster are listed in supplemental Table 4). (F) UMAP visualization of clustered cells featuring aggregated gene set expression of hallmark gene set "interferon-α response" split by condition (Camera GSEA: LT-HSC cluster *P* = 1.32e-07, ST-HSC cluster *P* = 5.46e-03). Volcano plot (right) shows differentially expressed genes in cluster "LT-HSC" with genes belonging to the hallmark pathway "interferon-α response" highlighted in red and labeled with gene name. (Differentially expressed genes between conditions per cluster are listed in supplemental Table 4). (G) Estimating the activity of transcription factors (TF) based on changes in abundance of their targets (input: full list of differentially expressed genes Csnk1a1$^{-/+}$ vs WT) as a proxy of their activity using method DoRothEA in cluster LT-HSC. Only transcription factors with activity scores >2.5/≤2.5 are shown here. Positive scores (red) signify increased activity of transcription factors in the Csnk1a1$^{-/+}$ condition and negative scores (blue) with decreased TF activity.

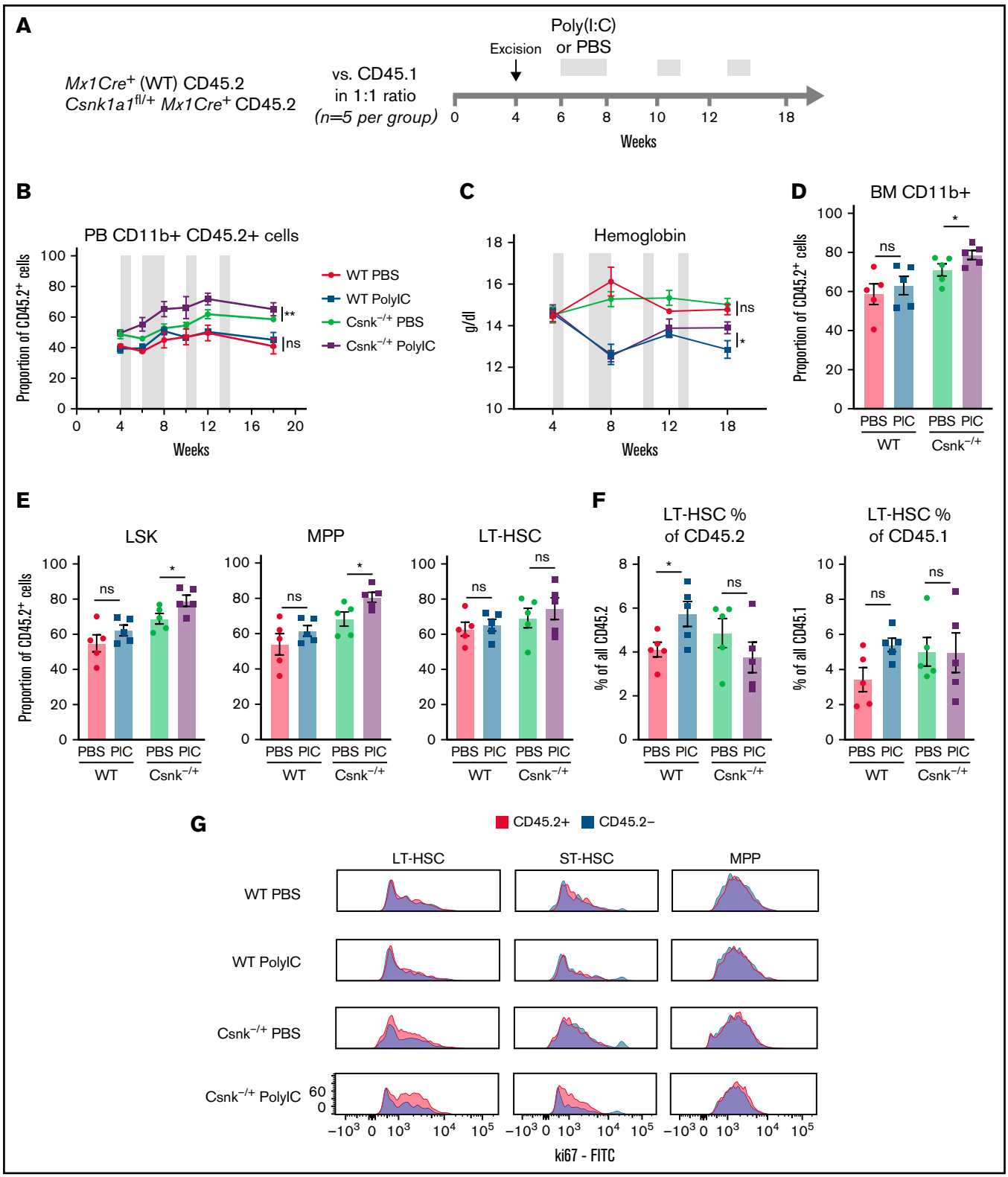

Figure 7. Competitive advantage of Csnk1a1 haploinsufficient HSCs is increased under exogenous inflammatory stress. (A) Experimental design. Competitive transplantation of whole bone marrow from *Mx1-Cre*$^{+}$ (WT) or *Csnk1a1*$^{fl/+}$ *Mx1-Cre*$^{+}$ (*Csnk*$^{-/+}$) mixed 1:1 with CD45.1^{+} ckit^{+} WT competitor cells (n = 5 each). After week 6, the WT and *Csnk*$^{-/+}$ groups were split into 2 groups receiving blocks of either 5 μg/g body weight poly(IC) or equal volume of phosphate-buffered saline (PBS) by intraperitoneal injection. (Injection blocks are marked in light gray: weeks 6-8, 11, and 13.) (B) Frequency of CD45.2^{+} cells in the CD11b^{+} myeloid fraction of peripheral blood. (Injection blocks are marked in light gray: weeks 6-8, 11, and 13.) (C) Hemoglobin values collected during transplant. (Injection blocks are marked in

Csnk1a1$^{+/-}$*Ctnnb1*$^{+/-}$ HSCs are outcompeted and (4) inflammation increases the competitive advantage of *Csnk1a1* haploinsufficient HSCs.

The genetic barcoding approach was implemented as a screening approach to identify any clonal advantage amid competing, genetically distinct cells in 1 microenvironment. Conventional competitive repopulation assays test only the growth of a genotype of interest vs a competitor (WT) cell population but do not provide clonal resolution. The competition of HSCs as tested here in the genetic barcoding approach does not occur in vivo but systematically compares the effect of haploinsufficient gene expression on HSC function. Genetic barcoding approaches have already been published that study steady-state hematopoiesis, but not competitive transplantation with single-cell resolution. We robustly recovered barcoded clones and observed a reduction of clonal complexity over time, which was in line with previously reported genetic barcoding in transplantation models.[25,37] Clones of all genotypes engrafted successfully, albeit not in equal proportions in the 9 mice analyzed. This was unexpected as the different genotypes engrafted as floxed but not excised alleles, and we confirmed that the gene expression was still comparable to that of WT cells (unexcised gene). Thus the unequal distribution 4 weeks after transplantation may be related to temporary engraftment of progenitor cells from the transplant, which show stochastic fluctuation and exhaustion over time, or unrepresentative recovery of barcodes in sampled blood at this early time point. The dynamical systems model that we developed based on experimental data suggests that differences in cell numbers at engraftment play a less significant role in clonal evolution than inter-individual differences in cell properties of different genotypes (eg, response to environmental factors, intrinsic differences, differences in proliferation and self-renewal).

The genetic barcoding approach corroborated by the classic competitive transplantation revealed that *Csnk1a1* and *Egr1* haploinsufficient HSCs have the potential to clonally expand and to dominate hematopoiesis. In particular *Csnk1a1* haploinsufficient clones showed an increased competitive advantage in consecutive transplantations.

Single cell transcriptome analysis of *Csnk1a1* haploinsufficient HSCs compared with WT revealed the most significant changes in the most primitive HSC compartment: LT-HSCs were expanded, and most differentially expressed genes were found in HSCs and megakaryocyte, erythroid and lymphoid progenitors. We summarize these differentially expressed genes as either HSC intrinsic, affecting proliferation and differentiation, or HSC extrinsic, which involve inflammatory processes.

Genes related to crucial HSC-intrinsic self-renewal and differentiation pathways such as cell cycle, oxidative phosphorylation, and Myc downstream signaling were particularly upregulated in the most primitive *Csnk1a1*$^{-/+}$ HSCs.[30,38,39] Significant enrichment of S-phase genes further supports this. *Csnk1a1* is known to exhibit cell cycle-dependent subcellular localization, including association with cytosolic vesicles and the nucleus during interphase, and with the mitotic spindle. β-Catenin is a substrate of *Csnk1a1*, and early-response genes, including *Myc* and c-*Jun* (both upregulated in our data) are targets of Wnt/β-catenin signaling. Although we do not observe a signature deregulation of Wnt/β-catenin signaling, reduced β-catenin levels were functionally shown to abolish the clonal advantage of *Csnk1a1* haploinsufficient cells. Interestingly, β-catenin levels were highest in HSCs from *Csnk1a1*$^{-/+}$*Apc*$^{-/+}$ mice (followed by *Csnk1a1*$^{-/+}$), whereas they were comparable between WT and *Csnk1a1*$^{-/+}$*Ctnnb1*$^{-/+}$. This demonstrates that the exact dosage of β-catenin is crucial in determining the clonal advantage, with too high or too low levels being detrimental to HSC function. These data indicate that Csnk1a1 functions as a negative regulator in the early stages of the G1-S transition and thus contributes to slow but steady clonal expansion.

Csnk1a1$^{-/+}$ immature noncommitted progenitors showed a characteristic downregulation of HSC-extrinsic mechanisms, such as immune response and inflammatory stress response. We thus hypothesized that *Csnk1a1*$^{-/+}$ HSCs are more robust to inflammatory stress, providing a selection advantage over WT cells. We can further demonstrate this, as *Csnk1a1*$^{-/+}$ HSCs, in direct competition with WT HSCs, gained a considerable advantage over WT HSCs under systemic low-dose inflammatory stress over time.

These HSC-extrinsic effects are particularly interesting as MDS co-occurs or is preceded by chronic inflammatory conditions such as autoimmune disease[35,40-43] or involves mutation of inflammation-inducible genes such as *SAMD9L*.[44-46] The germline mutations in SAMD9/9L in monosomy 7 and MDS encode gain-of-function proteins that appear to be overactivated in response to inflammatory stress. This effect causes downregulation of MAPK signaling and a corresponding proliferative arrest that results in transient aplasia and selects for outgrowth of mutant clones with loss of the mutant allele. *Csnk1a1* haploinsufficiency may represent the other side of this coin, whereby LT-HSCs fail to mount an appropriate inflammatory response and continue to proliferate inappropriately. Inflammatory cytokines and growth factors are elevated in patients with MDS alongside the innate immune response through toll-like receptor (TLR) signaling.[6,19,35] In del(5q) MDS haploinsufficiently expressed genes (eg, *RPS14*, *miR145*, *miR146*, and *TIFAB*[6,19,21]), are negative regulators of TLR signaling. Recent studies show that TLR-TRAF6–primed HSCs switch to noncanonical NF-κB signaling under chronic inflammatory conditions, demonstrating a long-term competitive advantage in this context.[19,20] In addition, Stoddart et al have recently shown in a murine model of del(5q) MDS with *Apc* and *Egr1* haploinsufficiency and loss of *Trp53* that alteration of the hematopoietic niche using alkylating agents significantly contributes to development of myeloid disease , highlighting the dependency of the (mutated) hematopoietic clone on its niche.[47]

Figure 7 (continued) light gray: weeks 6-8, 11, and 13.) (D) Proportion of CD45.2$^+$ cells in the bone marrow CD11b$^+$ fraction. (E) Frequency of CD45.2$^+$ cells in bone marrow LSK (Lin$^-$Sca1$^+$ckit$^+$), MPP (CD48$^+$CD150$^-$LSK), ST-HSC (CD48$^-$CD150$^-$ LSK), and LT-HSC (CD48$^-$CD150$^+$ LSK). Statistical significance tested by 1-way ANOVA with Dunnett's multiple-comparison test, comparing WT PBS to all other groups. Data are represented as the mean ± standard error of the mean (SEM). (F) The frequency of LT-HSC in either CD45.2$^+$ or CD45.1$^+$ compartment. Statistical significance for all panels was tested between poly(IC) and PBS conditions by a 1-tailed *t* test. Data are represented as the mean ± SEM. (G) Representative histograms of Ki67 expression in CD45.2+ or CD45.2$^-$ LT-HSCs, ST-HSCs, and MPPs of the experimental groups. Data represent mean ± SEM. (B-F) *$P < .05$, by 1-tailed Student *t* test.

The identified HSC-intrinsic and -extrinsic factors that contribute to a clonal advantage of *Csnk1a1*$^{-/+}$ HSCs may even be mechanistically linked. β-catenin is linked to TNF-α by NF-κB signaling, and can exert both negative and positive influences on the inflammatory response.[48,49] Based on functional experiments, we hypothesize that on the HSC level in *Csnk1a1* haploinsufficiency, β-catenin signaling, or direct *CSNK1A1* kinase effects are responsible for increased self-renewal and decreased inflammatory response, protecting from aging and extrinsic insult. At the level of multipotent progenitors, a mostly proproliferative effect may be assumed, leading to overall expansion of the genotype and outperformance of WT cells.

Unexpectedly, the combination of *Csnk1a1* and *Egr1* haploinsufficiency did not provide a greater competitive advantage than either alone. In particular for *Egr1*, the expansion advantage with increased self-renewal seems more variable than in *Csnk1a1*, suggesting that additional (extrinsic) cues are needed to spark the clonal advantage. It is very well possible that deletion of other genes on chromosome 5q is additionally necessary to drive expansion of the del(5q) clones by creating a favorable microenvironment.

Acknowledgments

The authors thank Remco Hoogenboezem for excellent support in processing raw sequencing data for downstream analysis.

This work was supported by grants from the MPN foundation (2017 MPNRF/LLS Award), a KWF Kankerbestrijding young investigator grant (11031/2017–1, Bas Mulder Award; Dutch Cancer Foundation) and a grant from the European Research Council (ERC) (deFIBER;ERC-StG 757339) to R.K.S., and by a grant from the NIH (R01 HL082945) to B.L.E. T.H.B., I.C. and R.K.S. are part of the clinical research unit CRU344 supported by the German Research Foundation (DeutscheForschungsgemeinschaft, DFG). I.C. and R.K.S. are members of the E:MED Consortia Fibromap, funded by the German Ministry of Education and Science (BMBF). I.C. was supported by an IZKF grant (E8-15). U.S.A.S. was supported by a research fellowship from the IMF University of Münster (ST521701) and by a research fellowship from the German Research Foundation DFG (STA 1648/1-1).

Authorship

Contribution: U.S.A.S. designed and performed the experiments, performed the biocomputational analyses, analyzed the results, and wrote the manuscript; F.T., R.L., A.B.W., G.S.C., N.B.L, A.S., and T.S. developed the biocomputational tools, performed the biocomputational analysis, interpreted the results, and reviewed the manuscript; I.A.M.S., S.N.R.F., M.E.M., S. Schmitz, M.A.E., S.M.-H., B.B., H.F.E.G., E.M.J.B., D.R., J.E.P., S. Sood, D.H., and T.H.B. performed the experiments, analyzed and interpreted the data, discussed the data, and reviewed the manuscript; I.G.C., B.L.E., and R.K.S. obtained funding, designed the study, performed the experiments, analyzed the data, and wrote the manuscript; and all authors provided critical analysis of the manuscript.

Conflict-of-interest disclosure: B.L.E. has received research funding from Celgene, Deerfield, and Novartis and consulting fees from GRAIL. He serves on the scientific advisory boards and holds equity in Skyhawk Therapeutics, Exo Therapeutics, and Neomorph Therapeutics, none of which are directly related to the content of this article. Remaining authors have no competing financial interests.

ORCID profiles: F.T., 0000-0001-8905-6657; H.F.E.G., 0000-0001-6138-8916; A.B.W., 0000-0003-1650-2710; S.S., 0000-0003-1188-2750; N.B.L., 0000-0003-2530-4329; D.R., 0000-0001-5122-861X; T.H.B., 0000-0002-9677-3723; T.S., 0000-0001-9686-9197; I.G.C., 0000-0003-2890-8697; B.L.E., 0000-0003-0197-5451.

Correspondence: Rebekka K. Schneider, Aachen University, Pauwelsstrasse 30, 52074 Aachen, Germany; e-mail: reschneider@ukaachen.de.

References

1. Schneider RK, Ademà V, Heckl D, et al. Role of casein kinase 1A1 in the biology and targeted therapy of del(5q) MDS. *Cancer Cell.* 2014;26(4):509-520.
2. Bello E, Pellagatti A, Shaw J, et al. CSNK1A1 mutations and gene expression analysis in myelodysplastic syndromes with del(5q). *Br J Haematol.* 2015;171(2):210-214.
3. Heuser M, Meggendorfer M, Cruz MMA, et al. Frequency and prognostic impact of casein kinase 1A1 mutations in MDS patients with deletion of chromosome 5q. *Leukemia.* 2015;29(9):1942-1945.
4. Hosono N, Makishima H, Mahfouz R, et al. Recurrent genetic defects on chromosome 5q in myeloid neoplasms. *Oncotarget.* 2017;8(4):6483-6495.
5. Polprasert C, Schulze I, Sekeres MA, et al. Inherited and somatic defects in DDX41 in myeloid neoplasms. *Cancer Cell.* 2015;27(5):658-670.
6. Ebert BL. Molecular dissection of the 5q deletion in myelodysplastic syndrome. *Semin Oncol.* 2011;38(5):621-626.
7. Järås M, Miller PG, Chu LP, et al. Csnk1a1 inhibition has p53-dependent therapeutic efficacy in acute myeloid leukemia. *J Exp Med.* 2014;211(4):605-612.
8. Wang J, Fernald AA, Anastasi J, Le Beau MM, Qian Z. Haploinsufficiency of Apc leads to ineffective hematopoiesis. *Blood.* 2010;115(17):3481-3488.
9. Qian Z, Chen L, Fernald AA, Williams BO, Le Beau MM. A critical role for Apc in hematopoietic stem and progenitor cell survival. *J Exp Med.* 2008;205(9):2163-2175.

10. Bidère N, Ngo VN, Lee J, et al. Casein kinase 1α governs antigen-receptor-induced NF-kappaB activation and human lymphoma cell survival. *Nature.* 2009;458(7234):92-96.
11. Elyada E, Pribluda A, Goldstein RE, et al. CKIα ablation highlights a critical role for p53 in invasiveness control. *Nature.* 2011;470(7334):409-413.
12. Min IM, Pietramaggiori G, Kim FS, Passegué E, Stevenson KE, Wagers AJ. The transcription factor EGR1 controls both the proliferation and localization of hematopoietic stem cells. *Cell Stem Cell.* 2008;2(4):380-391.
13. Joslin JM, Fernald AA, Tennant TR, et al. Haploinsufficiency of EGR1, a candidate gene in the del(5q), leads to the development of myeloid disorders. *Blood.* 2007;110(2):719-726.
14. Ebert BL, Pretz J, Bosco J, et al. Identification of RPS14 as a 5q- syndrome gene by RNA interference screen. *Nature.* 2008;451(7176):335-339.
15. Schneider RK, Schenone M, Ferreira MV, et al. Rps14 haploinsufficiency causes a block in erythroid differentiation mediated by S100A8 and S100A9. *Nat Med.* 2016;22(3):288-297.
16. Ebert BL. Deletion 5q in myelodysplastic syndrome: a paradigm for the study of hemizygous deletions in cancer. *Leukemia.* 2009;23(7): 1252-1256.
17. Lindsley RC, Ebert BL. Molecular pathophysiology of myelodysplastic syndromes. *Annu Rev Pathol.* 2013;8(1):21-47.
18. Lane SW, Sykes SM, Al-Shahrour F, et al. The Apc(min) mouse has altered hematopoietic stem cell function and provides a model for MPD/MDS. *Blood.* 2010;115(17):3489-3497.
19. Barreyro L, Chlon TM, Starczynowski DT. Chronic immune response dysregulation in MDS pathogenesis. *Blood.* 2018;132(15):1553-1560.
20. Muto T, Walker CS, Choi K, et al. Adaptive response to inflammation contributes to sustained myelopoiesis and confers a competitive advantage in myelodysplastic syndrome HSCs. *Nat Immunol.* 2020;21(5):535-545.
21. Ribezzo F, Snoeren IAM, Ziegler S, et al. Rps14, Csnk1a1 and miRNA145/miRNA146a deficiency cooperate in the clinical phenotype and activation of the innate immune system in the 5q- syndrome. *Leukemia.* 2019;33(7):1759-1772.
22. Cheung AF, Carter AM, Kostova KK, et al. Complete deletion of Apc results in severe polyposis in mice. *Oncogene.* 2010;29(12):1857-1864.
23. Lee SL, Tourtellotte LC, Wesselschmidt RL, Milbrandt J. Growth and differentiation proceeds normally in cells deficient in the immediate early gene NGFI-A. *J Biol Chem.* 1995;270(17):9971-9977.
24. Heidel FH, Bullinger L, Feng Z, et al. Genetic and pharmacologic inhibition of β-catenin targets imatinib-resistant leukemia stem cells in CML. *Cell Stem Cell.* 2012;10(4):412-424.
25. Lu R, Neff NF, Quake SR, Weissman IL. Tracking single hematopoietic stem cells in vivo using high-throughput sequencing in conjunction with viral genetic barcoding. *Nat Biotechnol.* 2011;29(10):928-933.
26. Verovskaya E, Broekhuis MJC, Zwart E, et al. Heterogeneity of young and aged murine hematopoietic stem cells revealed by quantitative clonal analysis using cellular barcoding. *Blood.* 2013;122(4):523-532.
27. Koelle SJ, Espinoza DA, Wu C, et al. Quantitative stability of hematopoietic stem and progenitor cell clonal output in transplanted rhesus macaques receiving transplants. *Blood.* 2017;129(11):1448-1457.
28. Zijlmans JM, Visser JW, Laterveer L, et al. The early phase of engraftment after murine blood cell transplantation is mediated by hematopoietic stem cells. *Proc Natl Acad Sci USA.* 1998;95(2):725-729.
29. Luis TC, Naber BAE, Roozen PPC, et al. Canonical wnt signaling regulates hematopoiesis in a dosage-dependent fashion. *Cell Stem Cell.* 2011; 9(4):345-356.
30. Murphy MJ, Wilson A, Trumpp A. More than just proliferation: Myc function in stem cells. *Trends Cell Biol.* 2005;15(3):128-137.
31. Holland CH, Szalai B, Saez-Rodriguez J. Transfer of regulatory knowledge from human to mouse for functional genomics analysis. *Biochim Biophys Acta Gene Regul Mech.* 2020;1863(6):194431.
32. Essers MAGG, Offner S, Blanco-Bose WE, et al. IFNalpha activates dormant haematopoietic stem cells in vivo. *Nature.* 2009;458(7240):904-908.
33. Haas S, Hansson J, Klimmeck D, et al. Inflammation-induced emergency megakaryopoiesis driven by hematopoietic stem cell-like megakaryocyte progenitors. *Cell Stem Cell.* 2015;17(4):422-434.
34. Esplin BL, Shimazu T, Welner RS, et al. Chronic exposure to a TLR ligand injures hematopoietic stem cells. *J Immunol.* 2011;186(9):5367-5375.
35. Sallman DA, List A. The central role of inflammatory signaling in the pathogenesis of myelodysplastic syndromes. *Blood.* 2019;133(10):1039-1048.
36. Grover A, Sanjuan-Pla A, Thongjuea S, et al. Single-cell RNA sequencing reveals molecular and functional platelet bias of aged haematopoietic stem cells. *Nat Commun.* 2016;7(1):11075.
37. Yu K-R, Espinoza DA, Wu C, et al. The impact of aging on primate hematopoiesis as interrogated by clonal tracking. *Blood.* 2018;131(11): 1196-1206.
38. Wilson A, Laurenti E, Trumpp A. Balancing dormant and self-renewing hematopoietic stem cells. *Curr Opin Genet Dev.* 2009;19(5):461-468.
39. Delgado MD, León J. Myc roles in hematopoiesis and leukemia. *Genes Cancer.* 2010;1(6):605-616.
40. Al Ustwani O, Ford LA, Sait SJN, et al. Myelodysplastic syndromes and autoimmune diseases–case series and review of literature. *Leuk Res.* 2013; 37(8):894-899.
41. Gañán-Gómez I, Wei Y, Starczynowski DT, et al. Deregulation of innate immune and inflammatory signaling in myelodysplastic syndromes. *Leukemia.* 2015;29(7):1458-1469.

42. Oishi Y, Manabe I. Macrophages in age-related chronic inflammatory diseases. *NPJ Aging Mech Dis.* 2016;2(1):16018.

43. Beier F, Masouleh BK, Buesche G, et al. Telomere dynamics in patients with del (5q) MDS before and under treatment with lenalidomide. *Leuk Res.* 2015;39(11):S0145-2126(15)30380-5

44. Tesi B, Davidsson J, Voss M, et al. Gain-of-function SAMD9L mutations cause a syndrome of cytopenia, immunodeficiency, MDS, and neurological symptoms. *Blood.* 2017;129(16):2266-2279.

45. Thomas ME III, Abdelhamed S, Hiltenbrand R, et al. Pediatric MDS and bone marrow failure-associated germline mutations in SAMD9 and SAMD9L impair multiple pathways in primary hematopoietic cells. *Leukemia.* 2021;35(11):3232-3244.

46. Narumi S, Amano N, Ishii T, et al. SAMD9 mutations cause a novel multisystem disorder, MIRAGE syndrome, and are associated with loss of chromosome 7. *Nat Genet.* 2016;48(7):792-797.

47. Stoddart A, Wang J, Fernald AA, et al. Cytotoxic therapy-induced effects on both hematopoietic and marrow stromal cells promotes therapy-related myeloid neoplasms. *Blood Cancer Discov.* 2020;1(1):32-47.

48. Ma B, Hottiger MO. Crosstalk between Wnt/β-catenin and NF-κB signaling pathway during inflammation. *Front Immunol.* 2016;7:378.

49. Deng J, Miller SA, Wang H-Y, et al. beta-catenin interacts with and inhibits NF-kappa B in human colon and breast cancer. *Cancer Cell.* 2002;2(4):323-334.